

Liquidus Temperature: Assessing Standard Glasses for Furnace Calibration

October 2019

V Gervasio	CH Skidmore
JV Crum	JL George
BJ Riley	BA Stanfill
JD Vienna	AA Kruger

DISCLAIMER

This report was prepared as an account of work sponsored by an agency of the United States Government. Neither the United States Government nor any agency thereof, nor Battelle Memorial Institute, nor any of their employees, makes **any warranty, express or implied, or assumes any legal liability or responsibility for the accuracy, completeness, or usefulness of any information, apparatus, product, or process disclosed, or represents that its use would not infringe privately owned rights.** Reference herein to any specific commercial product, process, or service by trade name, trademark, manufacturer, or otherwise does not necessarily constitute or imply its endorsement, recommendation, or favoring by the United States Government or any agency thereof, or Battelle Memorial Institute. The views and opinions of authors expressed herein do not necessarily state or reflect those of the United States Government or any agency thereof.

PACIFIC NORTHWEST NATIONAL LABORATORY
operated by
BATTELLE
for the
UNITED STATES DEPARTMENT OF ENERGY
under Contract DE-AC05-76RL01830

Printed in the United States of America

Available to DOE and DOE contractors from the
Office of Scientific and Technical Information,
P.O. Box 62, Oak Ridge, TN 37831-0062;
ph: (865) 576-8401
fax: (865) 576-5728
email: reports@adonis.osti.gov

Available to the public from the National Technical Information Service
5301 Shawnee Rd., Alexandria, VA 22312
ph: (800) 553-NTIS (6847)
email: orders@ntis.gov <<https://www.ntis.gov/about>>
Online ordering: <http://www.ntis.gov>

Liquidus Temperature: Assessing Standard Glasses for Furnace Calibration

October 2019

V Gervasio
JV Crum
BJ Riley
JD Vienna

CH Skidmore
JL George
BA Stanfill
AA Kruger

Prepared for
the U.S. Department of Energy
under Contract DE-AC05-76RL01830

Pacific Northwest National Laboratory
Richland, Washington 99354

Summary

Standard glasses are used to ensure accurate liquidus temperature measurements and furnace temperatures. The supply of the standard glasses used at Pacific Northwest National Laboratory (Standard Reference Material 773 [SRM-773]) has been depleted. Replacement standard glasses for furnace temperature verification and liquidus temperature measurement validation were fabricated and tested. Two glasses—ARG-1 and AmCm2-19—were fabricated in roughly 5 kg batches. The liquidus temperature of the glasses was measured and found to be consistent with those reported in literature.

The time required to reach a crystal fraction plateau was also experimentally determined as a function of heat-treatment temperature for both glasses. Recommendations are made for improving the method of furnace temperature verification.

Acknowledgments

The authors gratefully acknowledge the financial support provided by the U.S. Department of Energy Waste Treatment and Immobilization Plant Project.

The authors also thank Renee Russell, technical review and consultations on the work leading to this report. The authors thank Hans Brandal for quality assurance support and Veronica Perez for records management.

Acronyms and Abbreviations

ARG-1	Analytical Reference Glass-1
ASTM	American Society for Testing and Materials International
CF	crystal fraction
dC_F/dT	change in equilibrium crystal fraction as a function of temperature
GDL	Glass Development Laboratory
IC	ion chromatography
ICP-AES	inductively coupled plasma atomic emission spectroscopy
HLW	high-level waste
IHLW	immobilized high-level waste
ILAW	immobilized low-activity waste
LAW	low-activity waste
mass%	mass percent content
NIST	National Institute for Standards and Technology
OM	optical microscope/microscopy
Pt/Rh	platinum-10%rhodium
PNNL	Pacific Northwest National Laboratory
SD	standard deviation
SE	standard error
SLR	simple linear regression
SRM	Standard Reference Material
SwRI	Southwest Research Institute
T	temperature
T_a	temperature at which a glass is amorphous
T_c	temperature at which a glass has crystals
T_L	liquidus temperature
T_{L-CF}	T_L measured with the crystal fraction extrapolation method
T_{L-UT}	T_L measured with the uniform temperature furnace method
UT	uniform temperature
ΔT	difference between two temperatures
XRD	x-ray diffraction

Contents

Summary	iii
Acknowledgments.....	iv
Acronyms and Abbreviations.....	v
Contents	vi
1.0 Introduction	1
2.0 Experimental	3
2.1 Furnace Temperature Profiling.....	3
2.2 Glass Selection.....	3
2.3 Glass Batching and Melting	4
2.3.1 ARG-1	4
2.3.2 AmCm2-19.....	4
2.4 T_L Measurements.....	5
2.5 Heat Treatment Durations.....	8
3.0 Results and Discussion	9
3.1 ARG-1.....	9
3.1.1 Chemical Analysis	9
3.1.2 Liquidus Temperature.....	10
3.1.3 Heat-Treatment Duration.....	11
3.2 AmCm2-19.....	14
3.2.1 Chemical Analysis	14
3.2.2 Liquidus Temperature.....	14
3.2.3 Heat-Treatment Duration.....	16
4.0 Conclusions and Recommendations	21
5.0 References.....	23

Figures

Figure 1	ARG-1 air quenched glass (left) and thin slice for OM observation (right).....	3
Figure 2	AmCm2-19 glass after the second melt.	4
Figure 3	Pt/10%Rh boat used for heat treatments.	7
Figure 4	Schematic of how to cut the isothermal ARG-1 heat-treatment specimen for OM observation.	8
Figure 5	ARG-1 glass. Extrapolation of T_L using the mass% of CF detected by RD.....	11
Figure 6	ARG-1 CF as a function of time and temperature.	12
Figure 7	ARG-1 change in equilibrium CF as a function of temperature and time.....	13
Figure 8	Natural logarithm time to reach CF plateau vs. inverse temperature plot for ARG-1.	13
Figure 9	AmCm2-19 glass. Extrapolation of T_L using mass% of the CF detected by XRD.....	15
Figure 10	AmCm2-19 CF as a function of time and temperature.	17
Figure 11	AmCm2-19 change in equilibrium CF as a function of temperature and time.....	17
Figure 12	First derivative of the AmCm2-19 CF vs. temperature.	18
Figure 13	Standard and taller platinum boats used in the current study for 48-h heat treatments at 1200°C for AmCm2-19.....	19
Figure 14	Viscosity a function of temperature for AmCm2-19 glass.....	19
Figure 15	AmCm2-19 natural log of viscosity as a function of temperature.....	20

Tables

Table 1	Target composition of ARG-1 and AmCm2-19 glasses in mass fraction.	6
Table 2	Temperatures used for measuring T_L using the uniform temperature (UT) furnace method and the crystal fraction (CF) extrapolation method for ARG-1 (left) and AmCm2-19 (right).	7
Table 3	Temperatures used to test the thermodynamic equilibrium of ARG-1 (left) and AmCm2-19 (right) to determine ideal duration of heat treatments for T_L determination.	8
Table 4	Chemical analysis results of ARG-1. Measured values are compared to target values and to historical values, which are also reported.	9
Table 5	ARG-1 T_L determination using UT furnace method. T_a and T_c are highlighted in blue.	10
Table 6	ARG-1 T_L determination using the CF method.	10
Table 7	ARG-1 liquidus temperatures measured and reported in literature by the UT and CF methods.	11
Table 8	Crystal fraction in heat-treated specimens of ARG-1 as a function of temperature and time to determine the thermodynamic equilibrium.	12
Table 9	AmCm2-19 chemical analysis results.	14
Table 10	AmCm2-19 T_L determination using the UT furnace method. T_a and T_c are highlighted in blue.	15
Table 11	AmCm2-19 T_L determination using the CF method.	15
Table 12	AmCm2-19 liquidus temperatures measured and reported in literature by the UT and CF methods.	16
Table 13	Crystal fraction as mass% in heat-treated specimens of AmCm2-19 as a function of temperature and time to determine the thermodynamic equilibrium.	16
Table 14	Crystal content in mass% of triplicate heat treatments at 1200°C.	19

1.0 Introduction

The radioactive waste currently stored at the Hanford Site in southeastern Washington State will be vitrified into borosilicate glass for disposal. Vitrification using joule-heated ceramic melters will be accomplished by adding glass-forming chemicals to high-level waste (HLW)—the solid fraction high in radioactive isotopes—and as low-activity waste (LAW)—the liquid fraction that represents most of the waste that has a lower concentration of radioactive isotopes. Both HLW and LAW glasses will need to meet a set of compositional and physical property constraints to be efficiently processed and acceptable for disposal.

Given the known waste batch composition, models have been developed to predict the properties of the final glass compositions. One property of interest is the liquidus temperature (T_L), which is defined as the lowest temperature at which the melt and primary crystalline phase co-exist in thermodynamic equilibrium. The T_L is often used as a constraint to avoid possible crystal accumulation in the melter because crystals start forming at temperatures at which T is less than T_L . Crystal formation inside the melter or in the containers during the cooling of the molten glass could highly impact the cleanup operation by interfering with the proper function of the melter or by reducing the overall chemical durability of the residual glass. For example, an abundance of spinel crystals, which are rich in transition-metal oxides (e.g., NiO, FeO, Fe₂O₃, Cr₂O₃) and thus possibly found in HLW glasses, could interfere with the function of the melter itself by modifying the electrical conductivity of the molten glass, or they could precipitate in the melter riser, thereby obstructing pouring of the melt into canisters (Edwards et al. 2018; Matyas et al. 2017). Nepheline formation within the canisters during cooling is another crystalline phase that could have a high impact on the cleanup mission. Nepheline (NaAlSi₃O₈) is an aluminosilicate crystal that could easily form in high-alumina and high-soda glasses. It has a profound impact on glass chemical durability because nepheline formation results in an alumina- and silica-depleted residual glass matrix and, thus reduces the glass network connectivity and results in a less durable glass (Riley et al. 2018).

If one of these events—electrical interferences with the melter functioning (i.e., short circuiting), obstruction of the melter riser, and/or reduction of glass chemical durability—were to happen, the overall Hanford cleanup mission would be delayed, and the end cost increased. Thus, it is extremely important to predict and prevent such eventualities with the development and implementation of mathematical models that predict and avoid these possibilities. Therefore, studying the T_L is one of the routine measurements conducted to support development of the property-composition model.

Various methods are available for measuring T_L and the choice depends on glass properties such as viscosity, volatility, T_L itself, and lab capabilities. The most commonly used methods are 1) the uniform temperature (UT) furnace method, 2) the crystal fraction (CF) extrapolation method, and 3) the gradient temperature furnace method. Regardless of the chosen method, measuring T_L requires the furnace temperature to be as accurate as possible. Thus, the *Standard test method for determining liquidus temperature of waste glasses and simulated waste glasses* (ASTM C1720-2017) requires furnaces used for T_L measurements to be profiled and checked for accuracy using a standard glass of “known” T_L , either a Standard Reference Material (SRM) produced by the National Institute for Standards and Technology (NIST) or a standard glass traceable to a round robin study (Riley et al. 2011). This last step is extremely important when comparing data measured by different laboratories. To date, PNNL has used SRM-773, a transparent soda-lime-silica glass, produced by NIST and Analytical Reference Glass (ARG)-1 subject to a round robin study (Riley et al. 2011). Unfortunately, NIST has

discontinued the production of this glass and the batch of ARG-1 used in the round robin study was used up, making it necessary to find a substitute that meets the needs of the laboratory.

Moreover, the ASTM C1720-17 procedure suggests that the typical heat-treatment duration for temperatures $\geq 900^{\circ}\text{C}$ should be 24 ± 2 h, but the procedure states that the exact time could be subject to change on a per-glass basis. In this study, the crystal fraction was studied as a function of temperature and time to investigate the onset of thermodynamic equilibrium at different temperatures.

In this work, two glasses were tested for potential use as standards for furnace profiling—ARG-1 and a simulated americium/curium glass (AmCm2-19) (Riley et al. 2011) as well as of a function of temperature and time on the onset of thermodynamic equilibrium between the melt and primary phase crystals.

2.0 Experimental

2.1 Furnace Temperature Profiling

The furnace used for the current study went through the rigorous temperature profiling required by ASTM C1720-17 using the remaining PNNL SRM-773 glass stock.

For the ASTM C1720-17, each furnace used for T_L studies use a calibrated thermocouple (T/C) positioned close to the crucible used for the measurements. This ensures that the temperature recorded is the temperature to which the glass is exposed. The use of a standard glass provides an additional check for temperature accuracy. When there is a discrepancy between the reading of the T/C and the standard glass T_L measured, ASTM C1720-17 states that the stand inside the furnace must be repositioned until the T/C measurement is "... within the tolerance expected for the standard glass..." (Section 11.2, ASTM C1720-17). Every time this occurs, the furnace will need to be turned off, cooled and the inside stage repositioned. New 24 h isothermal heat treatments with the standard glass will need to be performed and the measured T_L compared with that of the standard glass. If the T_L measured is outside the standard glass tolerance, the process needs to be repeated until the two values are within tolerance.

2.2 Glass Selection

The two glasses selected for consideration were ARG-1 and AmCm2-19, a simulated americium/curium glass (Riley et al. 2011).

ARG-1 is a dark glass rich in Fe, Na, B, Al, and Ca, whose primary crystalline phase is spinel (Smith 1993), all of which are often found in HLW glasses. ARG-1 has a T_L value of $\sim 1030^\circ\text{C}$. However, the dark color of ARG-1 makes the detection of crystals via OM difficult, requiring the preparation of thin slices prior to observation (Figure 1). The ARG-1 slice preparation process and the difficulty in detecting the spinel crystals increases the labor time and requires skilled technicians.



Figure 1. ARG-1 air quenched glass (left) and thin slice for OM observation (right).

AmCm2-19 is an amber-colored glass rich in rare earth oxides, whose primary crystalline phase is a lanthanide borosilicate. AmCm2-19 has a T_L value of $\sim 1225^\circ\text{C}$. Despite its T_L value being higher than that of most HLW and LAW glasses, AmCm2-19 has been recognized as being a good candidate for profiling the T_L furnace because of its steep crystallization slope (i.e., the

change in equilibrium CF as a function of temperature ($dC_F/dT = -0.1786$) and optical transparency (Figure 2). These characteristics make this glass an easy glass to analyze for crystals, thus providing an option for evaluating furnace temperature accuracy near the higher temperature end of the spectrum for waste glass T_L studies.



Figure 2. AmCm2-19 glass after the second melt.

2.3 Glass Batching and Melting

2.3.1 ARG-1

A large stock of ARG-1 glass that was prepared in 1993 (Smith 1993) and stored as powder is available at the PNNL. In accordance with ASTM C1720-17, the glass to be used for T_L measurements must be in small particles between 0.4 mm and 4 mm (+40/-5 mesh) instead of powder. Powder is thought to increase the risk of losing the samples if it boiled over the sides of the Pt/Rh boat. Therefore, the ARG-1 feed was melted and quenched on an Inconel 690 plate to obtain the required glass form that could then be properly sized using careful crushing and sieving.

Five kilograms of ARG-1 powdered frit (Smith 1993) was divided into smaller aliquots and melted at 1150°C for 1 h in a 500 mL Pt/10%Rh crucible that had a tight-fitting Pt/10%Rh lid. The molten glass then was poured onto an Inconel 690 plate and quenched. One sample was sent to Southwest Research Institute (SwRI), where the glass composition was analyzed via inductively coupled plasma atomic emission spectroscopy (ICP-AES) and compared to the target composition to determine if volatile elements had been lost during the melt (Table 1).

2.3.2 AmCm2-19

A total of 5 kg of AmCm2-19 glass was prepared following the target composition listed in Table 1. Oxides, carbonates, and boric acid were used to batch the glass. Five 1.6 kg dry chemical batches were prepared separately and then mixed in a V-Blender prior to the first melt. Aliquots of dry chemicals were added to a 500 mL Pt/10%Rh crucible that had a tight-fitting Pt/10%Rh lid and then melted at 1420°C for 1 h. The molten glass was then poured onto an Inconel 690 plate to cool and stored in a common container. After completing the first melt, the glass was crushed into a fine powder, mixed together, and melted a second time in ~500 g batches under the same conditions of the first melt. Three random samples of glass were chemically analyzed via ICP-AES of fused and dissolved specimens at the SwRI. The results were compared to the target composition from the round robin study (Table 9).

2.4 T_L Measurements

The T_L values of both glasses were measured using UT and CF methods at the 24 h standard heat-treatment time suggested by ASTM C1720-17. We compared our measurement results to results published in the literature.

Approximately 250 g of both ARG-1 and AmCm2-19 were sieved to particle sizes between 0.4 mm and 4 mm and washed by ultrasonic cleaning to remove fines following ASTM C1720-17 (ASTM 2017). About 3 g of each washed glass were loaded into a 1.2 × 1.2 × 1.2 cm Pt/10%Rh crucible (Figure 3) that had a tight-fitting lid. Each crucible was loaded into a pre-heated furnace at the target temperature and heat treated at isothermal equilibrium for 24 h.

Table 1. Target composition of ARG-1 and AmCm2-19 glasses in mass fraction.

Component	Glass ID	
	ARG-1	AmCm2-19
Al ₂ O ₃	0.04528	0.11900
B ₂ O ₃	0.08386	0.09300
BaO	0.00040	-
CaO	0.01529	-
Ce ₂ O ₃	-	0.09700
CeO ₂	-	-
Cr ₂ O ₃	0.00096	-
Cs ₂ O	-	-
CuO	0.00008	-
Er ₂ O ₃	-	0.08800
Eu ₂ O ₃	-	0.00300
Fe ₂ O ₃	0.13844	-
Gd ₂ O ₃	-	0.00800
K ₂ O	0.02589	-
La ₂ O ₃	-	0.24000
Li ₂ O	0.03259	-
MgO	0.00850	-
MnO ₂	0.02389	-
Na ₂ O	0.11355	-
Nd ₂ O ₃	-	0.06300
NiO	0.01030	-
P ₂ O ₅	0.00250	-
Pr ₂ O ₃	-	0.02500
SiO ₂	0.48580	0.22900
Sm ₂ O ₃	-	0.01500
SrO	0.00006	0.02000
TiO ₂	0.01120	-
ZnO	0.00014	-
ZrO ₂	0.00128	-
Sum	1.00000	1.00000



Figure 3. Pt/10%Rh boat used for heat treatments.

Heat-treatment temperatures for both the UT and CF methods are reported in Table 2. The furnace used had been previously profiled using NIST SRM-773 glass.

Table 2. Temperatures used for measuring T_L using the U) furnace method and the CF extrapolation method for ARG-1 (left) and AmCm2-19 (right).

ARG-1		AmCm2-19	
UT	CF	UT	CF
1026	851	1226	1129
1031	900	1229	1150
	949		1160
	999		1180
			1200

After each UT heat treatment, the ARG-1 samples were cut diagonally, and the mid-sections were prepared into thin slices of about 10 X 5 mm for OM observation (Figure 4). When crystals were observed, the furnace temperature was increased ($\Delta T \leq 10^\circ\text{C}$) and the heat treatment was repeated using a clean Pt/10%Rh boat loaded with more of the previously sieved and washed glass particles. This step was repeated until the heat-treated glass slice was found to be crystal free by OM. The average between the temperature at which the sample was found to be amorphous (T_a) and the closest temperature at which the sample was found to have crystals (T_c) was used to calculate T_L . A similar process was used to measure T_L for AmCm2-19, but the AmCm2-19 could be observed directly under the OM without having to prepare thin slices.

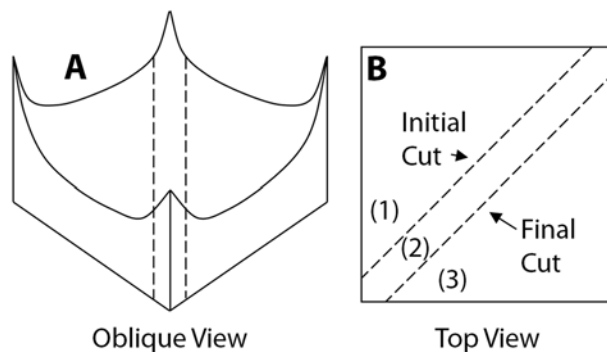


Figure 4. Schematic of how to cut the isothermal ARG-1 heat-treatment specimen for OM observation.

When using the CF method, both ARG-1 and AmCm2-19 were cut in half after each 24-h heat treatment and one half was prepared for X-ray diffraction (XRD) quantitative analysis using NIST 674b XRD standards (i.e., CeO₂ for ARG-1 and ZnO for AmCm2-19), and the other half was used for OM. T_L s were extrapolated using the crystal content of samples heat treated at different temperatures for 24 h. Differences in chemical compositions among the two glasses required the use of different temperatures for the isothermal heat treatments (Table 2).

2.5 Heat Treatment Durations

The ASTM C1720-17 procedure suggests that the typical heat-treatment duration for temperatures $\geq 900^\circ\text{C}$ should be 24 ± 2 h with the exact time subject to change on a per glass basis. Therefore, ARG-1 and AmCm2-19 were subjected to isothermal heat treatments at different temperatures and for different lengths of times to study the time required to reach the thermodynamic equilibrium at different temperatures. The temperatures used, three per glass, and durations, six per temperature, are reported in Table 3.

Table 3. Temperatures used to test the thermodynamic equilibrium of ARG-1 (left) and AmCm2-19 (right) to determine ideal duration of heat treatments for T_L determination.

UT Method			
Temperatures ($^\circ\text{C}$)		Times (h)	
ARG-1	AmCm2-19		
800	1150	2	16
850	1185	4	24
900	1200	8	48

Each heat treatment was run in triplicate. Approximately 3 g of each glass were loaded into $1.2 \times 1.2 \times 1.2$ cm Pt/10%Rh crucible that had a tight-fitting lid and heat treated for the stated time and temperature. CFs of the heat-treated specimens were determined quantitatively by XRD using NIST SRM-674b, which was added at a known concentration of ~ 5 mass%. The analyses were performed with a Bruker D8 Advance (Bruker AXS Inc.) instrument equipped with a Cu K $_{\alpha}$ target at 40 kV and 40 mA. The instrument had a LynxEye position-sensitive detector. The parameters used for data collection included a scan range of 5 to 70 $^\circ 2\theta$, a step size of 0.015 $^\circ 2\theta$, and a 1 s dwell at each step. EVA software (Bruker AXS Inc.) was used to identify phases present and TOPAS software (Bruker AXS Inc.) to quantify phases.

3.0 Results and Discussion

3.1 ARG-1

3.1.1 Chemical Analysis

ARG-1 powder feed stored at PNNL (Smith 1993) was re-melted to obtain a quenched glass. The final glass composition was analyzed and compared to the target composition to determine if volatile elements had been lost during the melt.

ARG-1 was chemically analyzed using ion chromatography (IC) and ICP-AES methods (anions and halogens by IC, metals by ICP-AES) of fused and dissolved specimens by SwRI. The results are reported in Table 4.

Table 4. Chemical analysis results of ARG-1. Measured values are compared to target values and to historical values, which are also reported.

Component	Measured Mass%	Target Mass%	% Difference	Average Measured from Riley et al. (2011) Mass%	% Difference between Current and Historical Measures
Al ₂ O ₃	4.592	4.528	1.40	4.730	-2.93
BaO	0.089	0.040	122.50	0.088	1.70
B ₂ O ₃	8.389	8.386	0.04	8.670	-3.24
CaO	1.567	1.529	2.49	1.430	9.58
Cr ₂ O ₃	0.095	0.096	-1.04	0.093	2.15
CuO	0.006	0.008	-25.00	0.004	50.00
Fe ₂ O ₃	15.012	13.844	8.44	14.000	7.23
Li ₂ O	3.208	3.259	-1.58	3.210	-0.08
MgO	0.868	0.850	2.12	0.860	0.93
MnO	1.847	2.389	-22.71	2.310	-20.06
NiO	1.043	1.030	1.21	1.050	-0.71
P ₂ O ₅	0.314	0.250	25.60	0.220	42.73
K ₂ O	2.656	2.589	2.59	2.710	-1.99
SiO ₂	47.704	48.580	-1.80	47.900	-0.41
Na ₂ O	11.438	11.355	0.73	11.500	-0.54
SrO	0.004	0.006	-33.33	0.004	0.00
TiO ₂	1.184	1.120	5.67	1.150	2.91
ZnO	0.023	0.014	64.29	0.020	15.00
ZrO ₂	0.135	0.128	5.47	0.130	3.85

The chemical analysis showed good agreement between measured and expected values. Values between $\pm 10\%$ are expected and considered normal for this type of analysis. All major components (with values ≥ 1 wt%) were found to be within 10% of the expected values. Also, all major components were found to be within $\pm 10\%$ of the literature reported values (Smith 1993; Table 4). No systematic variations in semi-volatile components (B, K, Na) were found to suggest excessive volatility during re-melting. Only six elements were outside the $\pm 10\%$ range. The $\sim 123\%$ difference in the Ba level, the -25% difference in the Cu level, the -23% difference in

the Mn level, -33% difference in the Sr level, and the 64% difference in the Zn level were due to how close they were to the detectability limit where accuracy is not very good. The P levels higher than the target quantity can be explained by the difficulty to measure P levels with the fusion methods used for these analyses.

3.1.2 Liquidus Temperature

ARG-1 T_L was measured using both the UT and CF methods with 24-h isothermal heat treatment. A total of eight 24-h heat treatments were conducted resulting in a T_c of 1026.1°C and a T_a of 1030.9°C with a ΔT of 4.9°C. T_L was therefore determined to be 1028.5°C \pm 2.4°C (Table 5). The reported 2.4°C value is the ΔT divided by two to compute an estimate of uncertainty because the T_L value could be anywhere within the ΔT range.

Table 5. ARG-1 T_L determination using UT furnace method. T_a and T_c are highlighted in blue.

Duration (hours)	Average Temperature (°C)	Crystal (Yes/No)
24	851.2	Y
24	900.5	Y
24	949.6	Y
24	997.5	Y
24	1017.3	Y
24	1024.2	Y
24	1026.1	Y (T_c)
24	1030.9	N (T_a)
T_L	1028.5	
ΔT :	4.9	

Six total heat treatments at different temperatures were used to extrapolate T_L using the CF method. Of these six, only the first five were used for the calculation because the crystal content of the highest temperature (1020°C) was below the quantitation limit of the XRD instrument; therefore, the data obtained were considered unreliable (Table 6). In each of the six samples, the crystalline phase detected by XRD was a transition-metal spinel, trevorite (NiFe₂O₄) was the best match. With the CF method, T_L was found to be 1030.8°C with a standard error (SE) of 10.6 with an R^2 of 0.98 (Figure 5). The 10.6°C SE was computed using a simple linear regression (SLR) model built to predict the glass liquidous temperature.

Table 6. ARG-1 T_L determination using the CF method.

Temperature (°C)	Crystal Content (wt%)
800	3.057
850	2.634
900	1.841
950	1.270
1000	0.31
1020	0.01

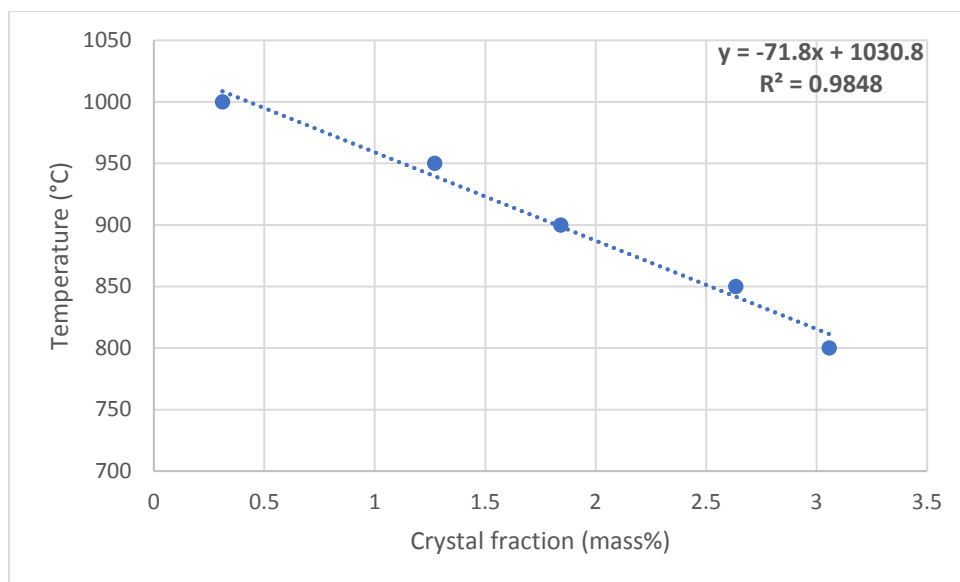


Figure 5. ARG-1 glass. Extrapolation of T_L using the mass% of CF detected by XRD.

The T_L of ARG-1 measured using both the UT furnace method (T_{L-UT}) and the CF extrapolation method (T_{L-CF}) were in accordance with what was previously found by Riley et al. (2011) during the round robin study. Indeed, in the current study, ARG-1 T_{L-UT} was $1028.5^\circ\text{C} \pm 2.4^\circ\text{C}$ ($\Delta T/2$) and T_{L-CF} was $1030.8^\circ\text{C} \pm 10.6^\circ\text{C}$ (SE) with an $R^2 = 0.985$ while during the round robin study, Riley et al. (2011) reported an average T_{L-UT} of $1036^\circ\text{C} \pm 6.9^\circ\text{C}$ standard deviation (SD), with a minimum $T_{L-UT} = 1024^\circ\text{C}$ and a maximum $T_{L-UT} = 1046^\circ\text{C}$, and a T_{L-CF} of $1041^\circ\text{C} \pm 14.2^\circ\text{C}$ (SD) (Table 7). The reported 6.9°C and 14.2°C SD are taken from Riley et al. (2011) and used as uncertainty estimate because the original data were not available to calculate the SE.

Table 7. ARG-1 liquidus temperatures measured and reported in literature by the UT and CF methods.

	T_{L-UT} measured	T_{L-UT} from literature	T_{L-CF} measured	T_{L-CF} from literature
ARG-1	1028.5°C $\pm 2.4^\circ\text{C}$ ($\Delta T/2$)	1036°C $\pm 6.9^\circ\text{C}$ (SD)	1030.8°C $\pm 10.6^\circ\text{C}$ (SE)	1041°C $\pm 14.2^\circ\text{C}$ (SD)

3.1.3 Heat-Treatment Duration

When the onset of thermodynamic equilibrium at different temperatures was investigated, the data showed a rapid increase of the CF until a plateau was reached (Table 8). The time required to reach the plateau depended on the temperature of the heat treatment and occurred sooner at higher temperatures—after ~ 4 h at 900°C , ~ 8 h at 850°C , and ~ 16 h at 800°C (Figure 6 and Figure 7). This effect was found to be best correlated in an Arrhenius-like relationship ($\ln[t]$ vs. T^{-1}), as shown in Figure 8.

Table 8. Crystal fractions in heat-treated specimens of ARG-1 as a function of temperature and time to determine the thermodynamic equilibrium.

Temperature	Time (h)					
	2	4	8	16	24	48
800°C	2.056	2.808	3.005	3.092	3.057	3.237
850°C	2.216	2.323	2.567	2.610	2.634	2.801
900°C	1.752	1.864	1.875	1.888	1.841	1.873

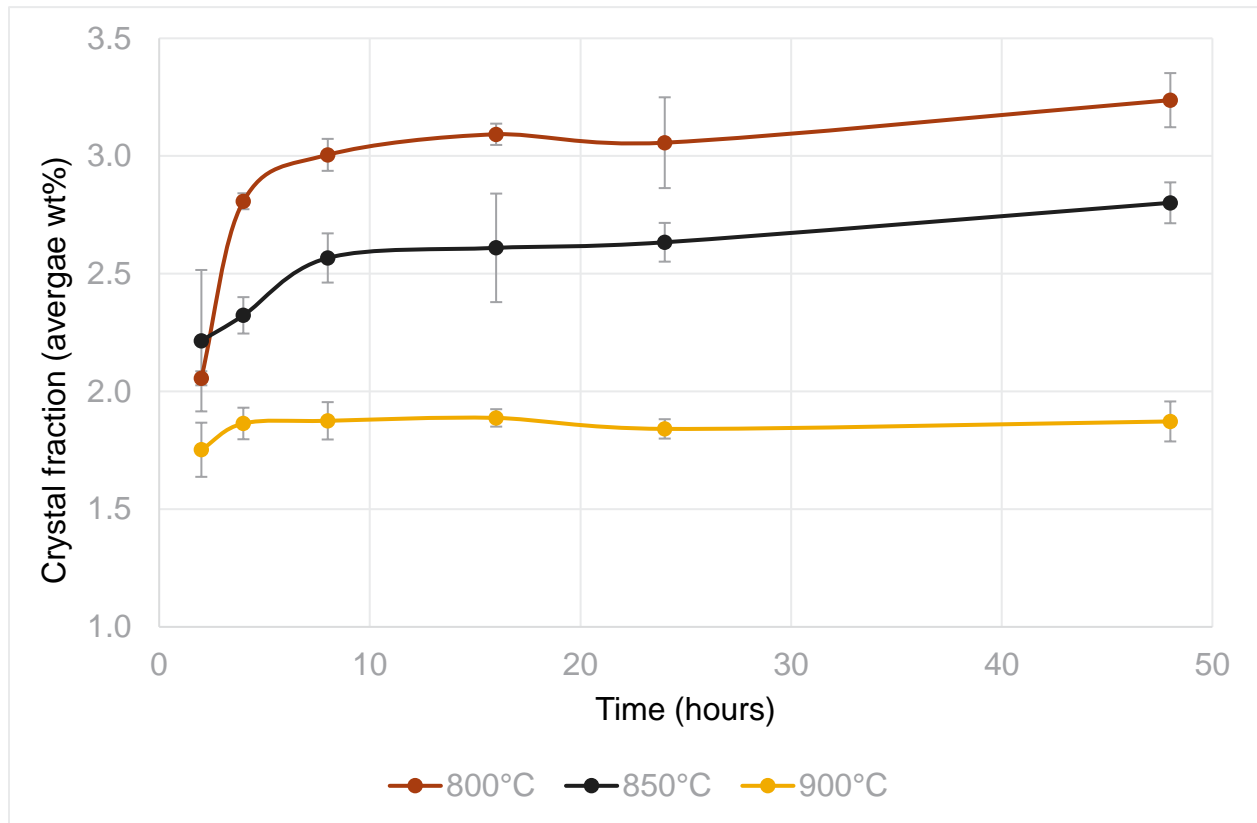


Figure 6. ARG-1 CF as a function of time and temperature. Each point was measured in triplicate, and the standard deviation of each point is reported.

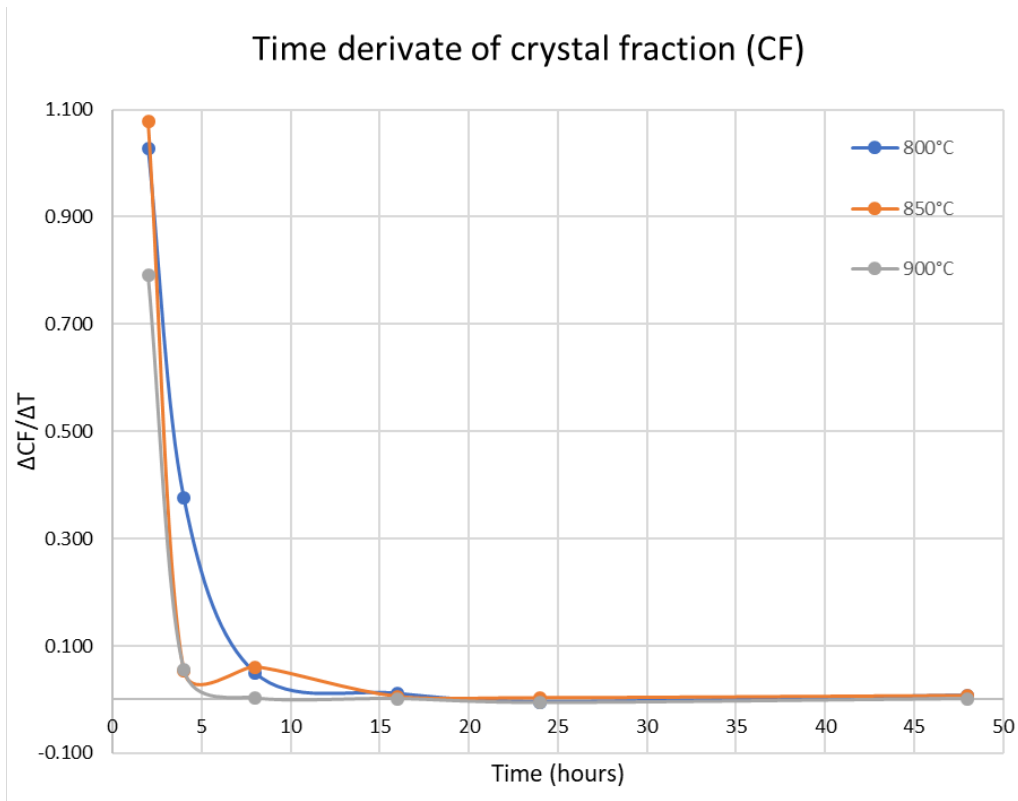


Figure 7. ARG-1 change in equilibrium CF as a function of temperature and time (first derivative).

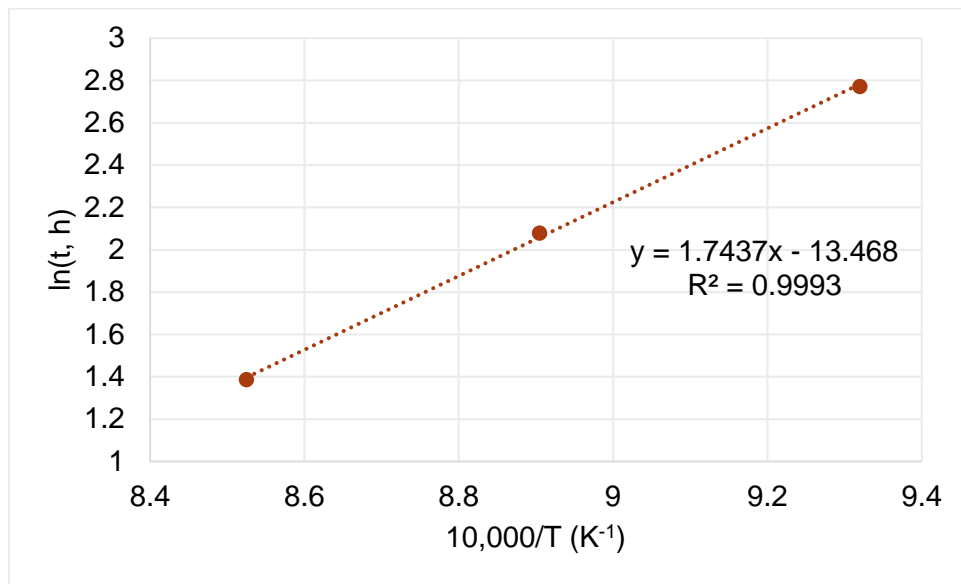


Figure 8. Natural logarithm time to reach CF plateau vs. inverse temperature plot for ARG-1.

3.2 AmCm2-19

3.2.1 Chemical Analysis

SwRI used the IC and ICP-AES methods to analyze fused and dissolved specimens of AmCm2-19. The results are compared to target values in Table 9. As mentioned for ARG-1, a deviation from the target between $\pm 10\%$ is considered normal in this type of analysis; therefore, the only analyte that significantly diverged from the target was Gd, which had an increase of 31% (Table 9). Decreases in the concentration of other lanthanides offset the increase in Gd₂O₃, resulting in a $\sim 2\%$ difference in total lanthanide oxide concentration ($\Sigma \text{Ln}_2\text{O}_3$). Only $\sim 2\%$ reduction in the semi-volatile B₂O₃ suggests a small impact of melting at such a high temperature (1420°C).

Table 9. AmCm2-19 chemical analysis results.

Component	Measured Mass%	Target Mass%	% Difference
Al ₂ O ₃	11.9	11.9	0.2
B ₂ O ₃	9.2	9.3	-1.6
Ce ₂ O ₃	9.8	9.7	1.5
Er ₂ O ₃	9.1	8.8	3.1
Eu ₂ O ₃	0.3	0.3	-9.3
Gd ₂ O ₃	1.0	0.8	30.9
La ₂ O ₃	22.2	24.0	-7.6
Nd ₂ O ₃	6.0	6.3	-4.2
Pr ₂ O ₃	2.6	2.5	3.1
SiO ₂	23.4	22.9	2.1
Sm ₂ O ₃	1.5	1.5	2.8
SrO	2.0	2.0	-1.9
$\Sigma \text{Ln}_2\text{O}_3$	52.6	53.9	-2.4

3.2.2 Liquidus Temperature

AmCm2-19 T_L was measured using the UT and CF methods with 24-h isothermal heat treatment. A total of eight 24-h heat treatments were conducted, resulting in a T_c of 1225.9°C and a T_a of 1229.3°C with a ΔT of 3.5°C (Table 10). The resulting T_L was 1227.6°C $\pm 1.7^\circ\text{C}$ ($\Delta T/2$) in accordance with the value of 1225°C $\pm 7.5^\circ\text{C}$ SD reported by Riley et al. (2011) (Table 12). Because the T_L value could be anywhere in the ΔT range, the reported 1.7°C value is the ΔT divided by two to compute an estimate of uncertainty.

We used five heat treatments at different temperatures to extrapolate T_L using the CF content method (Table 11). The crystalline phase detected by XRD was a lanthanum boron silicate crystal (Ln₃BSi₂O₁₀), and the T_L was 1218.7°C $\pm 2.7^\circ\text{C}$ (SE) with an R^2 of 0.99 (Figure 9). Riley et al. (2011) reported an average value of 1227°C $\pm 6.7^\circ\text{C}$ (SD) and a minimum value of 1220°C $\pm 5^\circ\text{C}$, which encompassed the range found in this study for a glass with the same target composition (Riley et al. 2011). The 2.7°C SE was computed using a SLR model built to predict the glass liquidous temperature. Because the intercept in the SLR model is an estimate of the glass liquidous temperature, the SE of the intercept estimate is reported along with it.

Table 10. AmCm2-19 T_L determination using the UT furnace method. T_a and T_c are highlighted in blue.

Duration (h)	Average Temperature (°C)	Crystals (Yes/No)
24	1125.7	Y
24	1150.6	Y
24	1159.2	Y
24	1178.8	Y
24	1199.0	Y
24	1219.7	Y
24	1225.9	Y (T_c)
24	1229.3	N (T_a)
T_L	1227.6	
ΔT :	3.5	

Table 11. AmCm2-19 T_L determination using the CF method.

Temperature (°C)	Crystal Content (Mass%)
1125.7	18.774
1159.0	11.741
1178.8	8.973
1185.00	6.289
1200.00	3.777

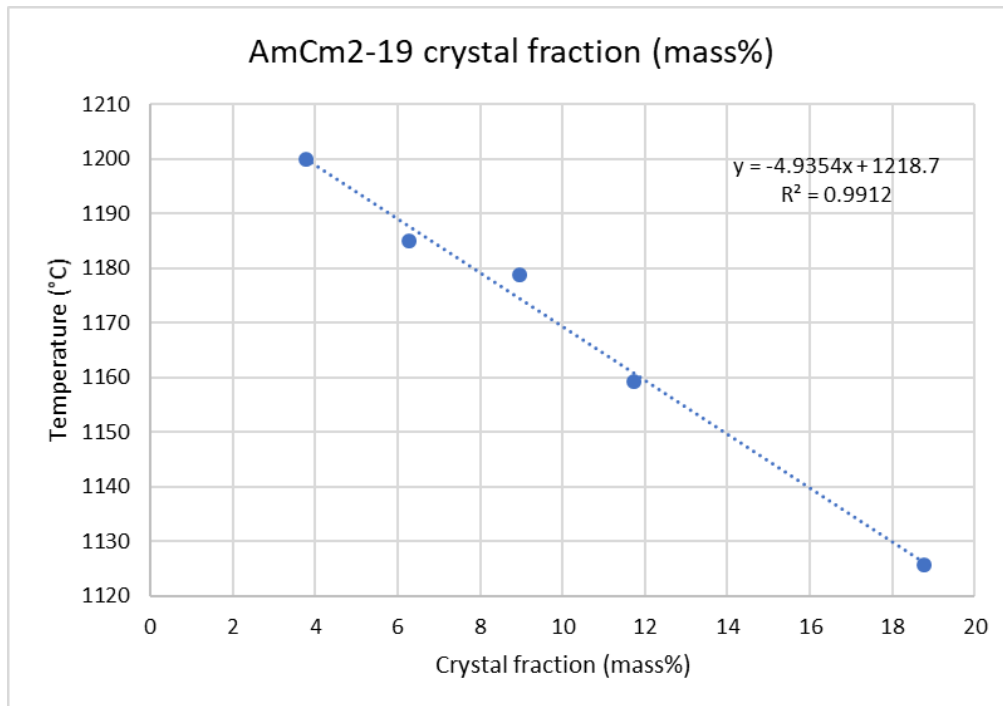


Figure 9. AmCm2-19 glass. Extrapolation of T_L using mass% of the CF detected by XRD.

Table 12. AmCm2-19 liquidus temperatures measured by the UT and CF methods and reported in literature.

	T_{L-UT} measured	T_{L-UT} from literature	T_{L-CF} measured	T_{L-CF} from literature
AmCm2-19	1227.6°C	1225°C	1218.7°C	1227°C
	±1.7°C ($\Delta T/2$)	±7.5°C (SD)	±2.7°C (SE)	±6.7°C (SD)

3.2.3 Heat-Treatment Duration

The onset of the thermodynamic equilibrium of AmCm2-19 was tested at three different temperatures: 1150°C, 1185°C, and 1200°C (Table 13).

Table 13. Crystal fraction as mass% in heat-treated specimens of AmCm2-19 as a function of temperature and time to determine the thermodynamic equilibrium.

Temperature	Time (h)					
	2	4	8	16	24	48
1150	8.415	8.719	9.289	10.261	10.228	10.214
1185	5.213	5.340	6.470	6.489	6.289	7.282
1200	2.380	2.382	3.026	3.668	3.777	4.136

At 1150°C, the CF increased up to 16 h then equilibrated. At 1185°C, the CF increased up to 8 h, then appeared to plateau and potentially increased from 24 to 48 h. At 1200°C, the CF increased steeply for the first 16 h and then increased very slowly to 48 h (Figure 10 and Figure 11).

The temperature derivative of the CF is compared to temperature in Figure 12. No correlation was found to relate crystallization rate or plateau time with temperature. However, very little additional crystallization occurred after 16 h at any of the test temperatures, suggesting a constant test time of ≥16 h.

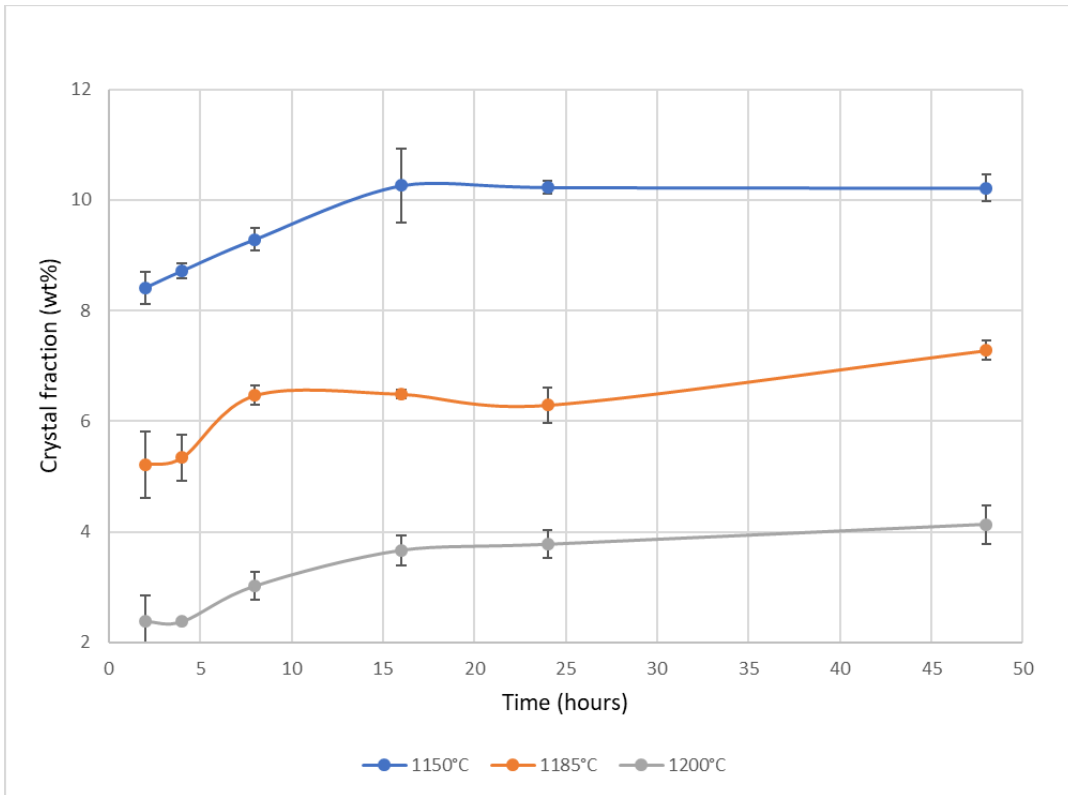


Figure 10. AmCm2-19 CF as a function of time and temperature. Each point was measured in triplicate, and the standard deviation of each point is reported.

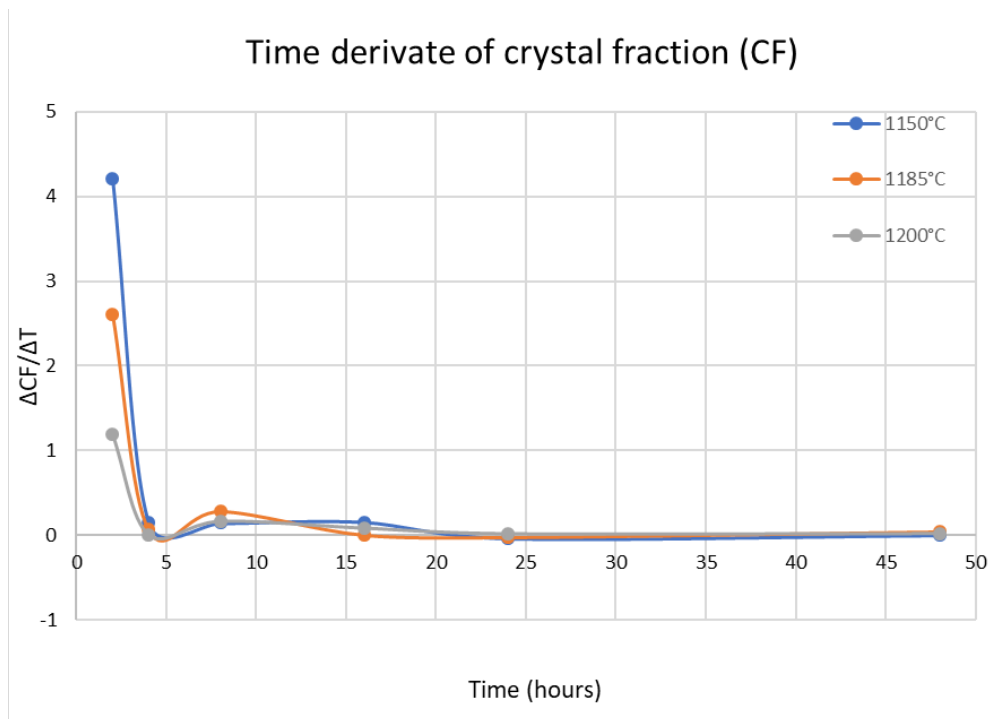


Figure 11. AmCm2-19 change in equilibrium CF as a function of temperature and time (first derivative).

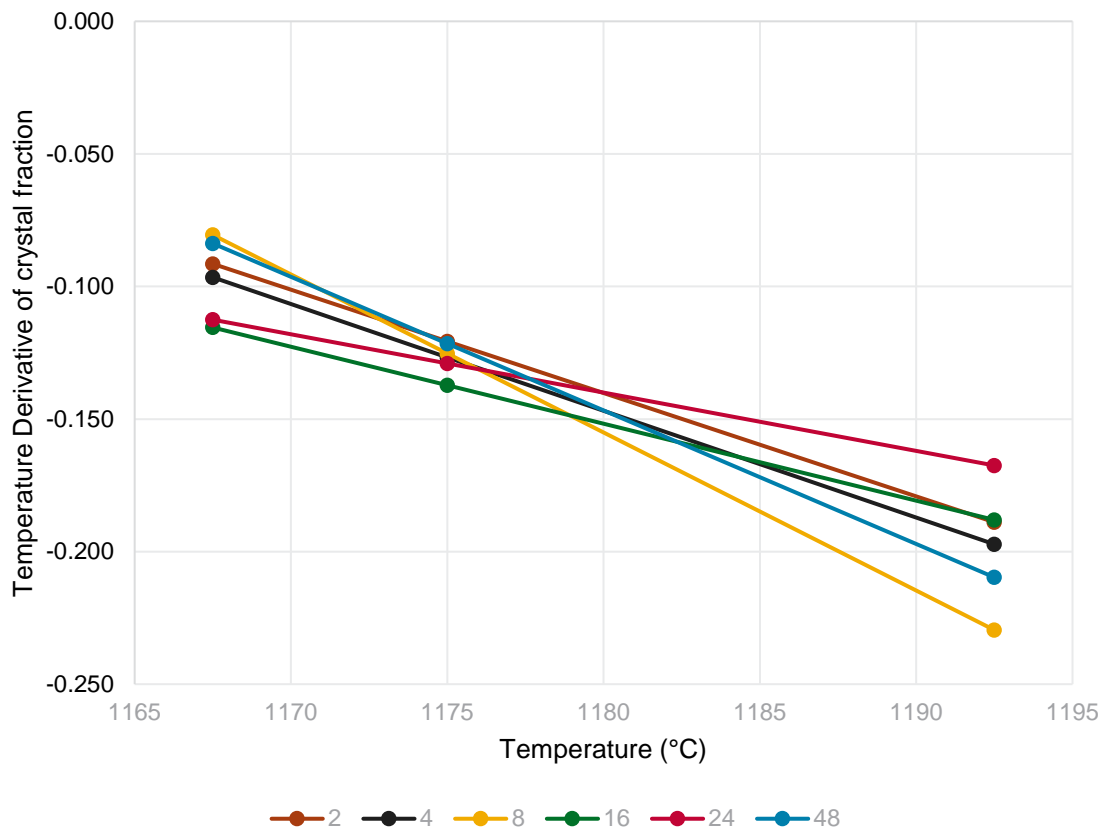


Figure 12. First derivative of the AmCm2-19 CF vs. temperature.

The lack of systematic change in crystallization rate and/or time to reach a CF plateau can be attributed to one or more phenomena such as 1) volatility during heat treatment changing the glass composition, 2) complicated nucleation and growth kinetics, 3) composition differences between samples, and/or 4) concurrent redox equilibration with crystal equilibration.

Multiple measurements at each time were performed at 1200°C to estimate the impacts of chemical heterogeneity (Table 14). This resulted in standard deviations between 0.01 and 0.5 wt%. To evaluate the potential impacts of volatility and nucleation, a larger Pt/10%Rh boat was used for a 48-h heat treatment (Figure 13). The average crystal content for the larger crucible was 2.7 ± 0.31 mass%, which is 37% lower than the value in smaller crucible (Table 14) (well beyond the 0.35 wt% standard deviation). The primary effect of crucible height is to change the surface area-to-volume ratio for the sample during heat treatment. This may affect nucleation, volatility, and redox equilibration. The volatility of semi-volatile components (e.g., alkalis, boron, etc.) can change the crystal equilibria, viscosity of the melt (Figure 14 and Figure 15), and viscosity/crystallization kinetics. Redox equilibrium can alter both the crystal equilibria (Hrma et al. 2006) and the kinetics.

Table 14. Crystal content in mass% of triplicate heat treatments at 1200°C.

Time (hours)	2	4	8	16	24	48	48 (tall Pt boat)
1 st	1.9	2.4	2.9	3.8	3.9	4.5	3.0
2 nd	2.4	2.4	2.9	3.4	3.5	3.9	2.5
3 rd	2.8	2.4	3.3	3.8	3.9	4.0	2.5
Average	2.4	2.4	3.0	3.7	3.8	4.1	2.6
STD	0.5	0.01	0.25	0.28	0.26	0.35	0.31



Figure 13. Standard and taller platinum boats used in the current study for 48-h heat treatments at 1200°C for AmCm2-19.

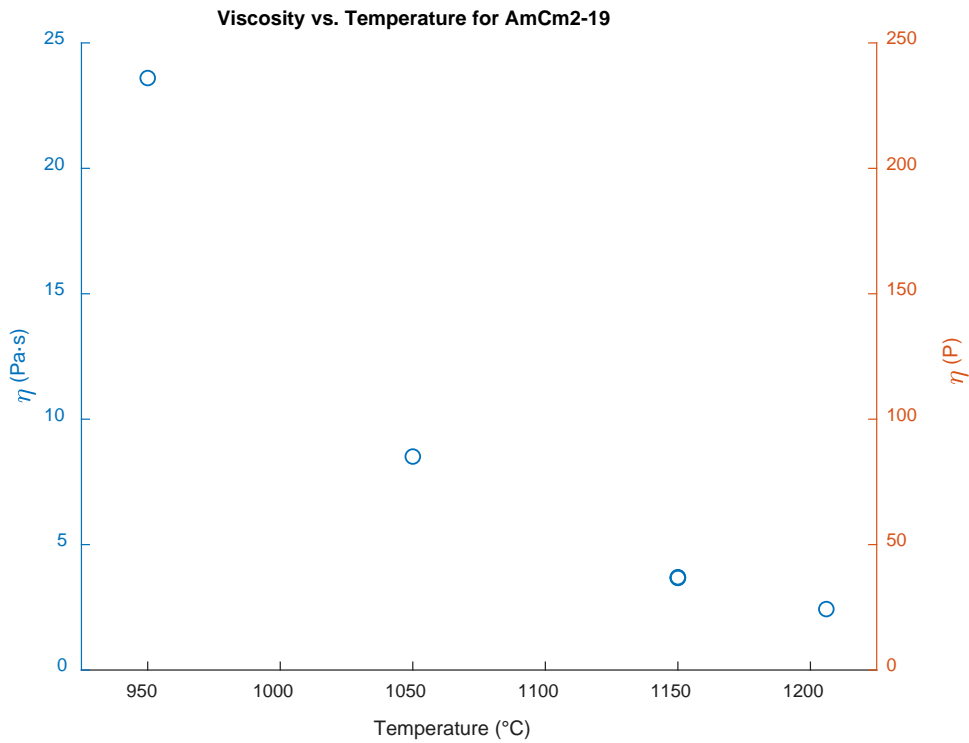


Figure 14. Viscosity a function of temperature for AmCm2-19 glass.

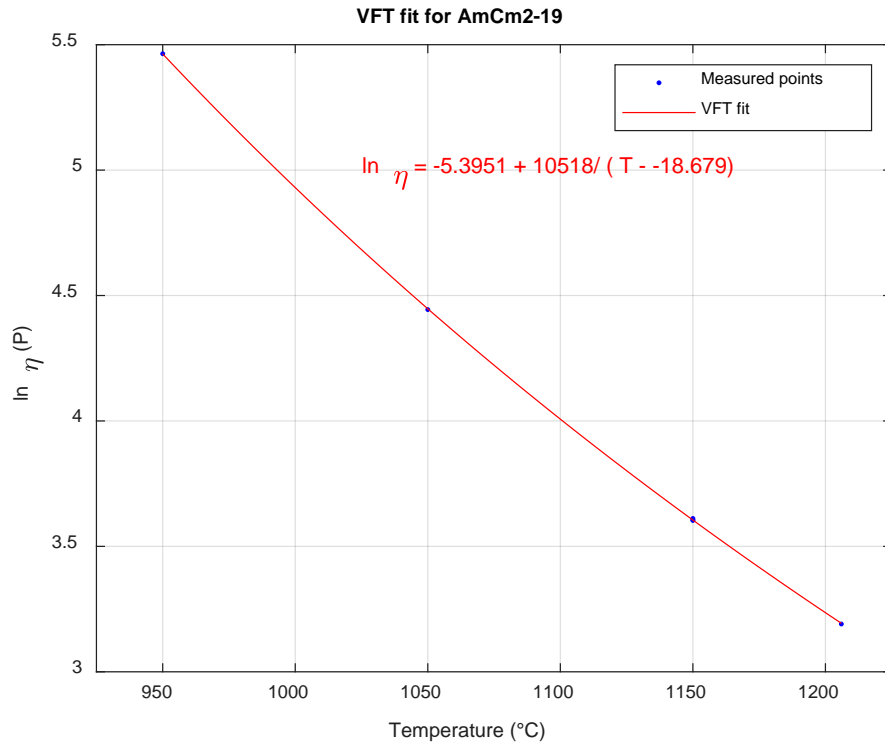


Figure 15. AmCm2-19 natural log of viscosity as a function of temperature.

4.0 Conclusions and Recommendations

According to the standard test method for determining T_L of waste glasses and simulated waste glasses (ASTM C1720-17 [ASTM 2017]), furnaces used for T_L measurements need to be profiled and checked for temperature accuracy using a glass of known T_L . This check can be performed either with an SRM glass produced by NIST or a glass traceable to a round robin study (ASTM C1720-17). For many years, PNNL used the NIST SRM-773 glass and then the ARG-1 glass. However, NIST discontinued the production of this glass making it necessary to find a substitute and the supplies of the round robin ARG-1 have been depleted. In this work, we chose two glasses—ARG-1 and AmCm2-19—both of which were included in a 2011 round robin study and included in the ASTM C1720-17.

The powdered ARG-1 glass from Smith (1993) was re-melted from the same larger batch used in the 2011 round robin (Riley et al. 2011), whereas AmCm2-19 was re-made from the laboratory chemicals to provide an adequate stockpile of the glass.

ARG-1 powder feed stored at PNNL was re-melted to obtain a quenched glass, and its chemical composition and T_L were verified to exclude changes in the original composition caused by volatilization loss during the melt. As for AmCm2-19, the new batched glass chemical composition and T_L were tested and compared to values reported in the literature.

Our results found that the glass compositions and the T_L of both ARG-1 and AmCm2-19 were comparable to the results found in the 2011 round robin study. From these two results, we concluded that both glasses could be satisfactorily used to profile the furnaces used for T_L measurements.

The furnace temperature profiling steps required by the ASTM C1720-17 are time consuming and, depending on the standard glass chosen, other factors may increase the time and difficulties linked with this process. For example, for an optically dark glass such as ARG-1, additional time is required to prepare the thin slices for OM observations or the spiked powder for XRD analysis, depending on the method used to measure T_L . For a glass such as AmCm2-19, which is transparent and with crystals that are easily detectable with OM, the preparation time for CF evaluation is notably lower than for ARG-1, but each time a new batch is made, additional steps will be needed to make sure that the glass has a “known T_L ” (e.g., one matching the 2011 round robin study or a new round robin study). The high cost of the glass and the verification tests will increase the overall project expenses and time required for processing.

Therefore, the process outlined in ASTM C1720-17 for profiling a furnace for T_L measurements is time consuming and expensive and also is subject to variability when a new standard glass batch needs to be made. The authors suggest investigating a new furnace temperature accuracy test for T_L measurements. For example, standard high-purity metals can be used to create a break-junction at a known melting temperature. Metals are commonly used for calibrating instruments such as differential thermal analyzers, differential scanning calorimeters, and thermo-mechanical analyzers. The use of metals would be advantageous for several reasons:

- Metals are relatively inexpensive.
- The composition would not vary when a new batch is needed (i.e., if the metals are purchased from a reliable chemical vendor).

- The test would require only few minutes until the metal melting temperature is reached and confirmed instead of the 24-h duration required when working with glasses.
- More than one metal could be analyzed at the same time with the correct apparatus.

For example, two or three metals with melting temperatures ranging from 1000°C to 1200°C could be chosen; for example, Cu (melting point 1083°C), Au (melting point 1064°C), or Nd (melting point 1010°C). Challenges would include designing a break-junction able to operate at high temperatures and overcoming the inconsistent oxidation rates of the metals; however, because of the advantages listed above, the authors think this alternative approach may warrant further investigation.

5.0 References

- ASTM (ASTM International). 2017. "Standard Test Method for Determining Liquidus Temperature of Immobilized Waste Glasses and Simulated Waste Glasses." ASTM C1720-17, West Conshohocken, Pennsylvania.
- Edwards MK, J Matyas, and JV Crum. "Real-Time Monitoring of Crystal Accumulation in the High-Level Waste Glass Melts with Electrical Conductivity Method." *International Journal of Applied Glass Science* 9 (2018) 1:42–51.
- Hrma P, JD Vienna, BK Wilson, TJ Plaisted, and SM Heald. "Chromium Phase Behavior in a Multi-Component Borosilicate Glass Melt." *Journal of Non-Crystalline Solids* 352 (2006):2114–2122.
- Matyas J, V Gervasio, SE Sannoh, and AA Kruger. 2017. "Predictive Modeling of Crystal Accumulation in the High-Level Waste Glass Melts Processing Radioactive Waste." *Journal of Nuclear Materials* 495. PNNL-SA-125881, Pacific Northwest National Laboratory, Richland, Washington.
- Riley BJ, P Hrma, JV Crum, JD Vienna, MJ Schweiger, CP Rodriguez, JV Crum, JB Lang, JC Marra, FC Johnson, DK Peeler, C Leonelli, AM Ferrari, I Lancellotti, J-L Dussossoy, RJ Hand, JM Schofield, AJ Connelly, R Short, and MT Harrison. 2011. "The Liquidus Temperature of Nuclear Waste Glasses: An International Round-Robin Study." *International Journal of Applied Glass Science* 2:321–333.
- Riley BJ, P Hrma, JV Crum, JD Vienna, MJ Schweiger, CP Rodriguez, and JP Peterson. 2018. "Liquidus Temperature in the Spinel Primary Phase Field: A Comparison between Optical and Crystal Fraction Methods." *Journal of Non-Crystalline Solids* 483:1–9.
- Smith GL. 1993. *Characterization of Analytical Reference. Glass-1 (ARG-1)*. PNL-8992, Pacific Northwest Laboratory, Richland, Washington.

Pacific Northwest National Laboratory

902 Battelle Boulevard
P.O. Box 999
Richland, WA 99354
1-888-375-PNNL (7665)

www.pnnl.gov